

Temperature dependence of the Raman-active B_{1g} and A_{1g} modes in $\text{YNi}_2\text{B}_2\text{C}$

T. Hirata and H. Takeya

National Research Institute for Metals, 1-2-1, Sengen, Tsukuba, Ibaraki 305, Japan

(Received 29 April 1997)

The Raman spectra of $\text{YNi}_2\text{B}_2\text{C}$ single crystals with a superconducting transition temperature $T_c = 14.2$ K have been measured in the temperature range 295–10 K. It turned out that the $B A_{1g}$ mode at 832 cm^{-1} whose broad linewidth was previously attributed to a strong electron-phonon coupling, actually consists of two components due to the isotope effect; the frequency ratio of each component approximates to $\sqrt{^{11}\text{B}/^{10}\text{B}} \approx 1.05$ of isotropic B masses. The 198 cm^{-1} B_{1g} mode due to Ni vibrations is fitted to a Fano-line profile, in order to derive the phonon parameters like frequency, linewidth, and asymmetry factor. The B_{1g} mode exhibits a normal temperature-dependent stiffening with no special change in the vicinity of T_c ; it also narrows revealing a deviation from a temperature-dependent anharmonic decay and a more symmetric character from 100 K with decreasing temperature. Based on no superconductivity-induced change in frequency and linewidth near T_c , it is concluded that there are no renormalization effects for the Ni B_{1g} mode, and that no strong electron-phonon coupling is operative in superconducting $\text{YNi}_2\text{B}_2\text{C}$. [S0163-1829(98)05106-6]

The intermetallic boro-carbide of $\text{YNi}_2\text{B}_2\text{C}$ crystallizes in body-centered tetragonal structure (space group $I4/mmm$; D^{17}_{2h}), and consists of Y-C layers separated by Ni_2B_2 sheets with lattice parameters of $a = 3.53 \text{ \AA}$ and $c = 10.57 \text{ \AA}$.¹⁻³ $\text{YNi}_2\text{B}_2\text{C}$ exhibits a well-defined superconducting transition at $T_c = 15.6 \text{ K}$.² To explore if $\text{YNi}_2\text{B}_2\text{C}$ among a new family of high- T_c intermetallic superconductors is a conventional electron-phonon superconductor, investigations of the phonons are essential as a matter of course.⁴⁻⁶ For tetragonal $\text{YNi}_2\text{B}_2\text{C}$ with $I4/mmm$, a symmetry-group analysis predicts the following irreducible representations at the Γ point with wave vector $k=0$.

$$\Gamma_{k=0} = A_{1g}(R) + B_{1g}(R) + 2E_g(R) + 3A_{2u}(IR) + 3E_u(IR) \\ + A_{2u} + E_u.$$

There are four Raman-active modes and six infrared-active modes along with two acoustic modes A_{2u} and E_u . The B_{1g} mode and one E_g mode are due to Ni vibrations, whereas another E_g mode and the A_{1g} mode are due to B vibrations. The Ni B_{1g} mode and the Ni E_g mode are observed at 198 and 282 cm^{-1} in polarized micro-Raman spectra of $\text{YNi}_2\text{B}_2\text{C}$,⁷ the $B E_g/B A_{1g}$ modes are observed at 470 and 832 cm^{-1} , respectively.

Hadjiev and co-workers⁷ have put forward a significant suggestion that the Ni vibrations that modulate the Ni-B bonds are of importance for the pairing state, and that renormalization effects may appear below T_c for the Ni B_{1g} mode at 198 cm^{-1} and the $B A_{1g}$ mode at 832 cm^{-1} . When the renormalization effects are provoked, the complex self-energy of the phonons near the Brillouin-zone center would undergo superconductivity-induced change.⁸ As a result of electron-phonon coupling, we can experimentally observe changes in frequency and linewidth of the phonon with frequency near the superconducting energy gap, i.e., $\omega \sim 2\Delta$.⁹ To our knowledge, however, no temperature dependence of the Raman spectra of $\text{YNi}_2\text{B}_2\text{C}$ has been reported, except the literature¹⁰ that focuses on a redistribution of light scattering

intensity at low frequencies between 10–200 K. In this situation, we are urged on variable-temperature Raman spectra of $\text{YNi}_2\text{B}_2\text{C}$ in a temperature range including T_c , so as to confirm if there are superconductivity-induced renormalization effects or any noticeable anomalies in the vicinity of T_c with respect to phonon properties of the Ni B_{1g} and/or $B A_{1g}$ modes in $\text{YNi}_2\text{B}_2\text{C}$.

Large single crystals of $\text{YNi}_2\text{B}_2\text{C}$ with dimensions of $6 \text{ mm } \phi \times 80 \text{ mm}$ in length were grown by a floating zone method as described elsewhere.¹¹⁻¹³ By x-ray diffraction as well as energy dispersive x-ray analysis, we found that the single crystals were of high quality and compositionally homogeneous with no second phase of YB_2C_2 . Magnetization measurements by a superconducting quantum interference device magnetometer identified the superconducting transition at $T_c = 14.2 \text{ K}$ and a small transition width of $\sim 0.5 \text{ K}$ for our single crystals. The orientation of the single crystals was determined by x-ray Laue photography, and a small piece of specimen was prepared so that it contains a surface perpendicular to the c axis.

Raman-scattering measurements were performed by a Dilor xy spectrometer with the 514.5 nm line of an Ar^+ ion laser (Coherent Inc., California, Innova 70-2) for excitation. The Raman spectra were recorded with a power of 50 mW in backscattering geometry; a liqN₂ cooled CCD multichannel detector (Photometrics Ltd, Princeton) was used to collect the scattered light. Low-temperature experiments were achieved by using a refrigerator unit (Daiken Ltd., Osaka, Cryokelvin UV2020-CL), which can cool the sample from room temperature down to 10 K with an accuracy of $\pm 1 \text{ K}$; the temperature fluctuation was slightly larger than $\pm 1 \text{ K}$ near T_c . Possible spectral changes were monitored over a temperature range between 295 and 10 K.

Figure 1 presents the Raman spectra of $\text{YNi}_2\text{B}_2\text{C}$ while cooling from 295 to 10 K. The Raman spectrum of $\text{YNi}_2\text{B}_2\text{C}$ at 295 K, which is characterized by the broad $B A_{1g}$ mode at $\sim 830 \text{ cm}^{-1}$ and the sharp Ni B_{1g} mode at $\sim 193 \text{ cm}^{-1}$, is in agreement with the polarized Raman spectrum from a micro-

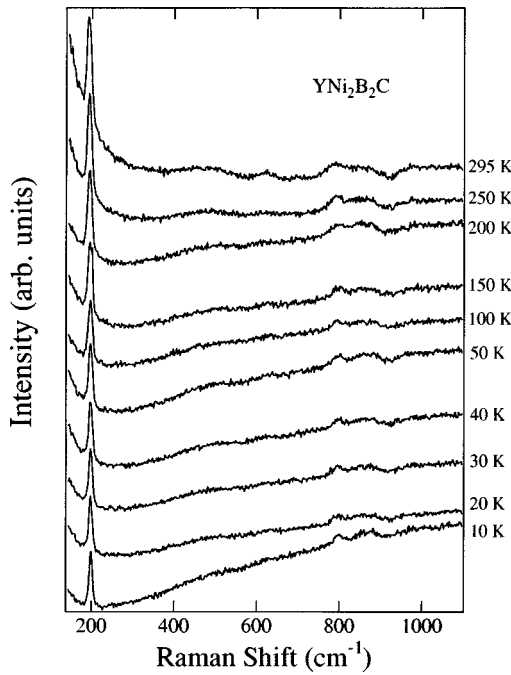


FIG. 1. The Raman spectra of $\text{YNi}_2\text{B}_2\text{C}$ while cooling from 295 to 10 K.

crystal of $\text{YNi}_2\text{B}_2\text{C}$ in the configuration $c(a,a)\bar{c}$.⁷ The $\text{Ni } E_g$ mode at 282 cm^{-1} and the $B E_g$ mode at 470 cm^{-1} are active in the (xz,yz) polarization geometry so that they are not observed in Fig. 1. A noticeable finding is that the 830 cm^{-1} A_{1g} mode appears to consist of two components and tends to be more resolved as the temperature is reduced. In Fig. 2, we depict the enlarged A_{1g} mode at 295 and 10 K, to demonstrate its two-component feature. The frequency ratio of each component approximates to $\sqrt{^{11}\text{B}/^{10}\text{B}} \approx 1.05$ of isotropic B masses with the abundance ratio $\approx 20/80$ for $^{10}\text{B}/^{11}\text{B}$, in conformity with the B isotope shift. No separation of the A_{1g} mode into the two isotropic counterparts has been mentioned previously.^{7,10} Rather, a large linewidth of the 810 cm^{-1} mode (118 cm^{-1} at 10 K) has been regarded as a conse-

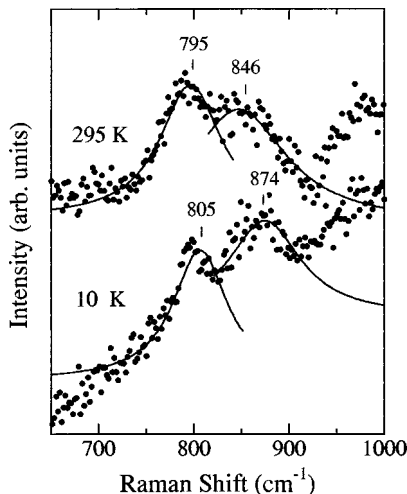


FIG. 2. The 832 cm^{-1} A_{1g} mode at 295 and 10 K, illustrating that this mode is composed of two components due to the B isotope effect.

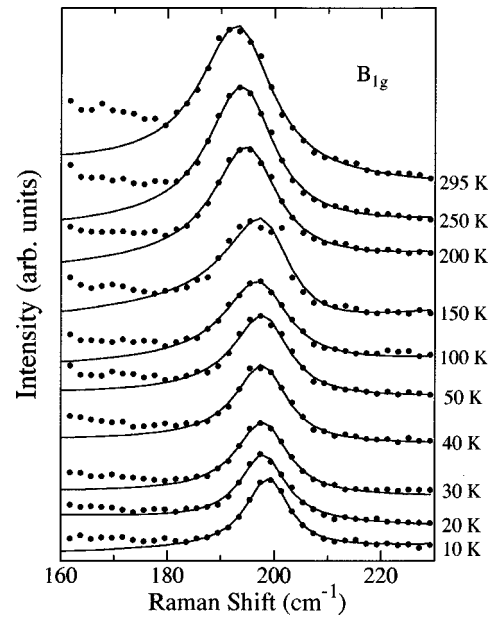


FIG. 3. The 198 cm^{-1} B_{1g} mode at different temperatures between 295 and 10 K; note that the Raman spectra (dots) are fitted to a Fano-line profile (solids lines).

quence of strong electron-phonon coupling.¹⁰ Due to the B-C bond shortening along the c axis upon cooling, the mode shifts downwards at 10 K.

Figure 3 depicts the temperature dependence of the 198 cm^{-1} B_{1g} mode along with fitting to a Fano-line profile. Obviously, the mode shifts upwards and decreases in intensity with cooling. The phonon parameters like frequency, full width at half maximum (FWHM) and asymmetry factor are obtained by fitting to the Fano-line profile,^{14–16} that is given by $I = I_0 [(\varepsilon + q)^2 / (1 + \varepsilon^2)] + \text{background}$, where $\varepsilon = (\omega - \omega_0) / \Gamma$, ω_0 is the frequency, Γ is the linewidth (FWHM) and q is a parameter that defines the asymmetry of the measured phonon profile; the background is represented in the form of $B\omega + C$ with B and C being adjustable parameters. We should like to mention that fitting converged properly, but note some disagreement between calculation and experiment at the lower-frequency part; the Rayleigh light is not of sufficient contribution in the frequency regime of $\sim 160 \text{ cm}^{-1}$ and thus its reason remains unexplained at present. Similar-sized frequencies and linewidths were also derived by fitting to Lorentzians as confirmed for the Raman-active models in $\text{YBa}_2\text{Cu}_3\text{O}_7$.¹⁷

In Fig. 4, the Raman shift, FWHM, Fano asymmetry factor q , and intensity of the 198 cm^{-1} B_{1g} mode are plotted as a function of temperature; we estimated the errors in each parameter, which are shown by the error bars. As for the relative change in each parameter with the errors under consideration, the mode frequency does not show any anomaly that can be readily relevant to the onset of superconductivity at $T_c \sim 14.2 \text{ K}$, but it simply exhibits a normal temperature dependence stiffening with decreasing temperature. The normal temperature dependence with no superconductivity-induced change has also been observed for the five A_g phonons of $\text{Y}_{0.56}\text{Pr}_{0.44}\text{Ba}_2\text{Cu}_3\text{O}_7$ (Ref. 18) and the 143 and 504 cm^{-1} modes in $\text{YBa}_2\text{Cu}_3\text{O}_7$.^{17,19} The FWHM of the mode decreases as the temperature is reduced; the tempera-

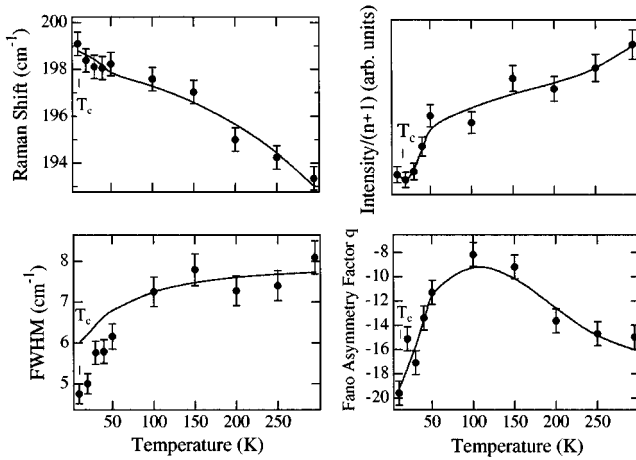


FIG. 4. The phonon parameters like frequency, full width at half maximum (FWHM) and asymmetry factor q are obtained by fitting to the Fano-line profile, and they are plotted as a function of temperature; the intensity of the mode, divided by the Bose-Einstein factor $(n+1)$, is plotted as well. Note that the solid line for the FWHM is due to the temperature-dependent anharmonic decay of the phonon (see text for details) whereas the other solid lines are only for guiding the eye. We estimated the errors in each parameter, which are shown by the error bars.

ture dependence is somewhat described by a temperature-dependent anharmonic decay of the Raman-active phonon with frequency ω and zero wave vector into two phonons with opposite wave vector between 295–100 K; $2\gamma(\omega, T) = 2\gamma(\omega, 0)[1 + 2n(\omega/2)] + \text{const}$, which is shown by a solid line with $2\gamma(\omega, 0)$ being an adjustable parameter,^{15,17,20} and the Bose factor $n = [\exp(\hbar\omega/kT) - 1]^{-1}$. Interestingly, there is a deviation from the temperature-dependent anharmonic decay from 100 down to 10 K. The intensity of the 198 cm^{-1} B_{1g} mode, divided by the Bose-Einstein factor $(n+1)$, continuously decreases exhibiting no specific change at T_c but with an accelerated decline below 100 K.

The Fano asymmetry factor q initially increases while cooling from 295 to 100 K, and then becomes more negative below 100 K amounting to a factor of ~ 2 . Similar initial increase in q has also been observed for the Raman mode at 120 cm^{-1} in $\text{YBa}_2\text{Cu}_3\text{O}_7$, which becomes more symmetric and narrow as well at $T_c = 93 \text{ K}$.¹⁷ Since a larger negative value represents a more symmetric lineshape, it follows that the Ni B_{1g} mode at 198 cm^{-1} becomes more symmetric below 100 K, due to the reduced interaction between the mode and superconducting quasiparticles.

The absence of superconductivity-induced renormalization effects for the Ni B_{1g} mode at 198 cm^{-1} as seen above, supports no strong electron-phonon coupling in superconducting $\text{YNi}_2\text{B}_2\text{C}$. In fact, tunneling spectroscopy has determined the superconducting energy gap of $\text{YNi}_2\text{B}_2\text{C}$ to be $\sim 2.3 \text{ meV}$ (18.5 cm^{-1}), providing a superconducting energy gap to T_c ratio near the BCS prediction of $2\Delta/kT_c = 3.5$ for a weak coupling superconductivity.^{21,22} It should be recalled that a new peak at $\sim 4.0 \text{ meV}$ in neutron scattering of $\text{YNi}_2\text{B}_2\text{C}$ in the Q range around $(0.525, 0, 8)$ is also consistent with the BCS prediction.²³ On the other hand, the specific-heat anomaly at T_c for $\text{YNi}_2\text{B}_2\text{C}$ provides $\Delta C_p/\gamma T_c = 3.6$ (γ is the coefficient of the electronic heat capacity), which is much higher than the BCS value of 1.43 for the weak-coupling limit, concluding that $\text{YNi}_2\text{B}_2\text{C}$ is a strong-coupling superconductor.^{24,25} However, no definite conclusion can be drawn about the entire electron-phonon coupling strength that is averaged over all phonons and at all k points in the Brillouin zone; note that the specific-heat data are sensitive to all phonons, which does not allow a direct comparison with the conclusion based on one specific phonon at the Γ point. No superconducting-gap-like feature was observed in our Raman spectra because it is expected to appear at $\approx 37 \text{ cm}^{-1}$ to reconcile with the BCS prediction of $2\Delta/kT_c = 3.5$. Besides, no detailed analysis has been made for the 832 cm^{-1} A_{1g} mode because of its isotope-induced complication. A study is requested on $\text{YNi}_2\text{B}_2\text{C}$ single crystals containing ^{11}B only, together with the temperature dependence of the $B A_{1g}$ mode at 832 cm^{-1} as well as the two Ni(B) E_g modes. This will promote a better understanding on the electron-phonon coupling strength in superconducting $\text{YNi}_2\text{B}_2\text{C}$.

In conclusion, the Raman spectra of $\text{YNi}_2\text{B}_2\text{C}$ single crystals have been measured in a temperature range of 295–10 K, focusing on the $B A_{1g}$ and the Ni B_{1g} modes at 832 cm^{-1} and 198 cm^{-1} , respectively. It is highlighted that the broad 832 cm^{-1} A_{1g} mode is not resultant due to a strong electron-phonon coupling but consists of two components due to the B isotope shift. The Ni B_{1g} mode at 198 cm^{-1} exhibits no noticeable anomalies in frequency, linewidth or Fano asymmetry factor in the vicinity of T_c . There is no presence of superconductivity-induced renormalization effects for the 198 cm^{-1} B_{1g} mode, indicating no strong electron-phonon coupling in superconducting $\text{YNi}_2\text{B}_2\text{C}$.

We acknowledge F. Fujishima of MST (Foundation for Promotion of Materials Science and Technology of Japan) for Raman-scattering measurements.

¹R. J. Cava, H. Takagi, B. Batlogg, H. W. Zandbergen, J. J. Krajewski, W. F. Peck, Jr., R. B. van Dover, R. J. Felder, T. Siegrist, K. Mizahashi, J. O. Lee, H. Eisaki, S. A. Carter, and S. Uchida, *Nature (London)* **367**, 146 (1994).

²R. J. Cava, H. Takagi, H. W. Zandbergen, J. J. Krajewski, W. F. Peck, Jr., T. Siegrist, B. Batlogg, R. B. van Dover, R. J. Felder, K. Mizahashi, J. O. Lee, H. Eisaki, and S. Uchida, *Nature (London)* **367**, 252 (1994).

³T. Siegrist, H. W. Zandbergen, R. J. Cava, J. J. Krajewski and W.

F. Peck Jr., *Nature (London)* **367**, 254 (1994).

⁴L. F. Mattheiss, T. Siegrist, and R. J. Cava, *Solid State Commun.* **8**, 587 (1994).

⁵W. E. Pickett and D. J. Singh, *Phys. Rev. Lett.* **72**, 3702 (1994).

⁶P. Dervenagas, M. Bullock, J. Zarestky, P. Canfield, B. K. Chao, B. Harmon, A. I. Goldman, and C. Stassis, *Phys. Rev. B* **52**, R9839 (1995).

⁷V. G. Hadjiev, L. N. Bozukov, and M. G. Baychev, *Phys. Rev. B* **50**, 16 726 (1994).

- ⁸R. Zeyher and G. Zwirgagl, *Z. Phys. B* **78**, 175 (1990).
- ⁹E. Altendorf, J. Chrzanowski, J. C. Irwin, A. O'Reilly, and W. N. Hardy, *Physica C* **175**, 47 (1991).
- ¹⁰A. P. Litvinchuk, L. Börjesson, N. X. Phuc, and N. M. Hong, *Phys. Rev. B* **52**, 6208 (1995).
- ¹¹H. Takeya, T. Hirano, and K. Kadowaki, *Physica C* **220**, 3256 (1996).
- ¹²H. Takeya, K. Kadowaki, K. Hirata, T. Hirano, and K. Togano, *J. Magn. Magn. Mater.* **157/158**, 611 (1996).
- ¹³H. Takeya, K. Kadowaki, K. Hirata, and T. Hirano, *J. Alloys Compd.* **245**, 94 (1996).
- ¹⁴E. Altendorf, X. K. Chen, J. C. Irwin, R. Liang, and W. N. Hardy, *Phys. Rev. B* **47**, 8140 (1993).
- ¹⁵B. Friedl, C. Thomsen, and M. Cardona, *Phys. Rev. Lett.* **65**, 915 (1990).
- ¹⁶K-M. Ham, J-T. Kim, R. Sooryakumar, and T. R. Lemberger, *Phys. Rev. B* **47**, 11 439 (1993).
- ¹⁷K. F. McCarty, J. Z. Liu, Y. X. Jia, R. N. Shelton, and H. B. Radousky, *Physica C* **192**, 331 (1992).
- ¹⁸K. F. McCarty, J. Z. Liu, Y. X. Jia, R. N. Shelton, and H. B. Radousky, *Phys. Rev. B* **46**, 11 958 (1992).
- ¹⁹R. M. Macfarlane, H. Rosen, and H. Seki, *Solid State Commun.* **88**, 843 (1993).
- ²⁰B. Friedl, C. Thomsen, E. Schönherr, and M. Cardona, *Solid State Commun.* **76**, 1107 (1990).
- ²¹T. Ekino, H. Fujii, M. Kosugi, Y. Zenitani, and J. Akimitsu, *Physica C* **235-240**, 2529 (1994).
- ²²G. T. Jeong, J. I. Kye, S. H. Chun, Z. G. Khim, W. C. Lee, P. C. Canfield, B. K. Cho, and D. C. Jonston, *Physica C* **253**, 48 (1995).
- ²³H. Kawano, H. Yoshizawa, H. Takeya, and K. Kadowaki, *Phys. Rev. Lett.* **77**, 4628 (1996).
- ²⁴H. Takeya, S. Miyamoto, K. Yamada, K. Nonose, and K. Kadowaki, *Physica C* **282-287**, 715 (1997).
- ²⁵C. Godart, L. C. Gupta, R. Nagarajan, S. K. Dhar, H. Noel, M. Potel, Chandan Mazumdar, Zakir Hossain, C. Levy-Clement, G. Schiffmacher, B. D. Padalia, and R. Vijayaraghavan, *Phys. Rev. B* **51**, 489 (1995).